

Color Text Fading Detection*

Runzhe Zhang^a, Eric Maggard^b, Yousun Bang^c, Minki Cho^c, Mark Shaw^b, Jan Allebach^a

^aSchool of Electrical and Computer Engineering, Purdue University, West Lafayette, IN 47906, U.S.A.

^bHP Inc., Boise, ID 83714, U.S.A.

^cHP Inc., Suwon City, KOREA.

Abstract

The text fading defect is one of the most common defects in electrophotographic printers; and it dramatically affects print quality. It usually appears in a significant symbol Region of Interest (ROI), easily noticed by a user on his or her print. We can detect text fading by the density reduction for the black and white printed symbol ROI. It is difficult to detect the color text fading only by density reduction, because the depleted cartridge may only cause the color distortion without density reduction in the color printed symbol ROI.

In our previous work with print quality defects analysis, the text fading detection method only works for black text fading defect detection [1]. Our new text fading method can detect the color text fading defect and predict the depleted cartridge. In this new text fading detection method, we use whole page image registration and the median threshold bitmap (MTB) matching method to align the text characters between the master and test symbol ROIs, because with the aligned text characters, it is easy to extract the difference between the master and the test text characters to detect the text fading defect. We use a support vector machine classifier to assign a rank to the overall quality of the printed page. We also use the gap statistic method with the K-means clustering algorithm to extract the different text characters' different colors to predict the depleted cartridge.

1. Introduction

Our new text fading detection method can detect the color text fading defect and predict the depleted cartridge. Figure 1 shows two examples of the color text fading defect in symbol ROIs: Figure 1 (a) shows an excellent print quality image; Figure 1 (b) shows a black text fading defect image; Figure 1 (c) shows a yellow text fading defect image. Here, the green text has become cyan in color. Previous text fading defect detection methods have been proposed, such as by ΔE value to detect the severity of text fading defects [1]. We updated this text fading detection method. Our new method not only can detect the severity of the text fading defect, but also can predict the depleted cartridge. In the depleted cartridge prediction part, we refer to a previous color fading detection method [2]. Besides, we optimize the text character alignment process to improve the efficiency of our algorithm. This symbol ROI text fading detection module is part of a larger effort to analyze print quality defects [3]. In our previous work, we designed a method to extract four different types of ROI from the input image, which are symbol, raster, vector, and

background ROI [4]. In this module, we only process the symbol ROIs. Figure 2 (b) shows the symbol ROIs based on the sample image Figure 2 (a). In each symbol ROI, we detect the text fading defect first, and extract the feature vector of the text fading defect. The feature vector is used to classify the rank of the text fading defect and to predict the depleted cartridge. Part of this feature vector will be used for the whole page classification.



Figure 1: Text fading sample images.

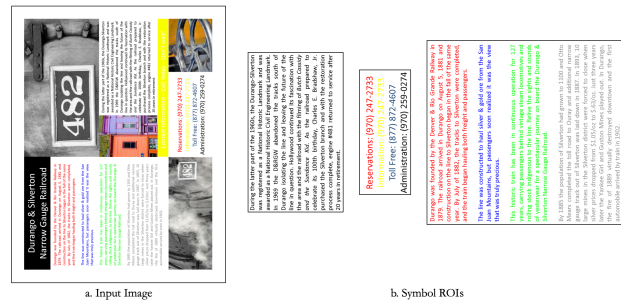


Figure 2: Symbol ROIs based on input image.

We will cover the details of the ROI extraction process and the evaluation results in the following sections.

2. Text fading detection and classification procedure

In this section, we introduce the details of our text fading detection and classification procedure. Figure 3 shows the overall pipeline of the proposed method. This procedure includes three parts: text character alignment, text fading classification, and prediction of the depleted cartridge.

The first part aligns the text characters between each scanned test symbol ROI and the corresponding master image symbol ROI. We use an image registration algorithm to spatially align the scanned test image symbol ROI and master image symbol ROI first. This image registration process

*Research supported by HP Inc., Boise, ID 83714

can roughly align the corresponding symbol ROIs, but it cannot achieve pixel-to-pixel accuracy alignment. We use the median threshold bitmap (MTB) [5] algorithm to align the corresponding text characters in the master and test symbol ROI. The second part detects the text fading defect. In this part, we calculate the ΔE value between the corresponding text characters in the test and master symbol ROIs in CIE $L^*a^*b^*$ color space. The statistics of the CIE $L^*a^*b^*$ values and the ΔE value are extracted to build the feature vector of the text fading defect in each symbol ROI to detect the text fading defect. The third part predicts the depleted cartridge of the printer. In this part, we use the gap statistic method with the K-means clustering algorithm to detect the number of text character colors. For each color text character, we can analyze the difference between master and test symbol ROI in CMYK color space to predict the depleted cartridge.

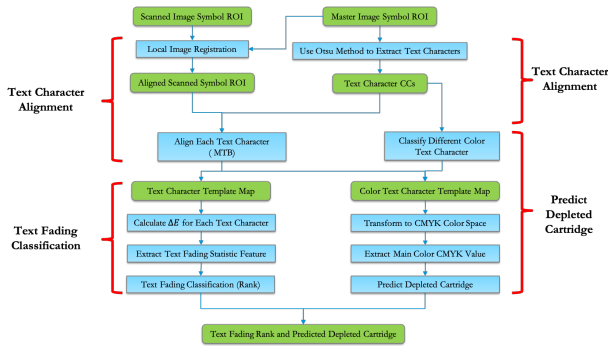


Figure 3: The overall pipeline of the symbol ROI text fading detection and classification.

We will introduce the details of the symbol ROI text fading detection and classification process in the following sections.

3. Text character alignment

Before we detect the text fading defect in the test image symbol ROI, we need to align the text characters because we need to compare the difference between the test and master text characters to determine whether there is a fading defect. This section includes two parts. The first part does the symbol ROI image registration, and the second part does the pixel to pixel text character alignment using the median threshold bitmap (MTB) method.

3.1 Symbol ROI image registration

A misalignment always exists in the scanned printed page compared to the master image after it is printed from a printer and scanned by the scanner. Figure 4 (a) shows an example of the misalignment between the master and the scanned test image. This misalignment must be removed before we do the text fading detection. One of the most common methods is the frequency-based approach, which calculates the phase correlation of two images in the Fourier domain [6]. In this project, there is a halftone pattern in the scanned image, and the frequency-based approach is not robust. Instead, we use a feature-based image registration method to remove the misalignment.

In the image registration process, the first step is to

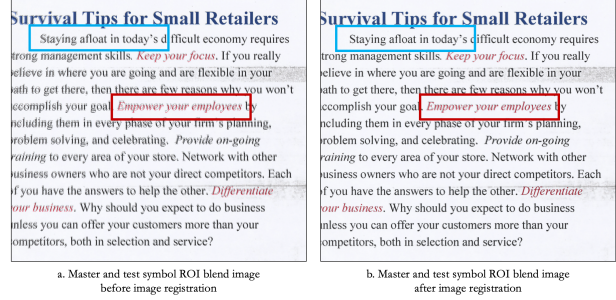


Figure 4: A master and test symbol ROI blend image before and after image registration.

convert the scanned test image and the master image to grayscale. In the next step, we use the SIFT method to detect the scale-space interest points with a 128-element descriptor in both the master and test images [7]. In the SIFT method, we use a Difference-of-Gaussian (DoG) pyramid to find all the local extrema, as shown in Equation 1. The function $G(x, y, k\sigma)$ is a variable scale Gaussian defined in Equation 2; k is the scale parameter, and it usually is 2; $ff(x, y, \sigma)$ is the Laplacian-of-Gaussian (LoG) of the image $I(x, y)$ [8]. We use these functions to find points that are locally maximum or locally minimum in the three-dimensional space $(x, y, k\sigma)$. For one extrema point, we need to consider 26 neighbors in the 3D neighborhoods.

$$D(x, y, \sigma) = [G(x, y, k\sigma) - G(x, y, \sigma)] * I(x, y) = ff(x, y, k\sigma) - ff(x, y, \sigma) \quad (1)$$

$$G(x, y, k\sigma) = \frac{1}{2\pi\sigma^2} \exp(-(x^2 + y^2)/2\sigma^2) \quad (2)$$

Because we use different scales σ across the DoG pyramid to detect the extrema point, we want to achieve greater precision in the localization of the extrema at a pixel-to-pixel level in the original image. In order to do this, we estimate the second-order derivatives of $D(x, y, \sigma)$ at the sampling points in the DoG pyramid. We can localize the extrema point with “sub-pixel” accuracy in the vicinity of where the DoG pyramid finds the extrema point. The Taylor series expansion of $D(x, y, \sigma)$ in the vicinity of $\vec{x}_0 = (x_0, y_0, \sigma_0)^T$, which was found to be the location of an extrema in the DoG pyramid, is shown in Equation 3. The variable \vec{x} is the incremental deviation from \vec{x}_0 ; J is the gradient vector estimated at \vec{x}_0 , as shown in Equation 4; H is the Hessian at \vec{x}_0 , as shown in Equation 5. Taking the derivative of both sides of the Taylor series expansion with respect to the vector variable \vec{x} , we get the result shown in Equation 6.

$$D(\vec{x}) \approx D(\vec{x}_0) + J^T(\vec{x}_0)\vec{x} + \frac{1}{3}\vec{x}^T H(\vec{x}_0)\vec{x} \quad (3)$$

$$J(\vec{x}_0) = \left(\frac{\partial D}{\partial x}, \frac{\partial D}{\partial y}, \frac{\partial D}{\partial \sigma} \right)^T \quad (4)$$

$$H(\vec{x}_0) = \begin{bmatrix} \frac{\partial^2 D}{\partial x^2}, & \frac{\partial^2 D}{\partial x \partial y}, & \frac{\partial^2 D}{\partial x \partial \sigma} \\ \frac{\partial^2 D}{\partial y \partial x}, & \frac{\partial^2 D}{\partial y^2}, & \frac{\partial^2 D}{\partial y \partial \sigma} \\ \frac{\partial^2 D}{\partial \sigma \partial x}, & \frac{\partial^2 D}{\partial \sigma \partial y}, & \frac{\partial^2 D}{\partial \sigma^2} \end{bmatrix} \quad (5)$$

$$\begin{aligned} 0 &\approx J(\vec{x}_0) + H(\vec{x}_0) \vec{x} \\ \vec{x} &= -H^{-1}(\vec{x}_0) \cdot J(\vec{x}_0) \end{aligned} \quad (6)$$

Once we have the local extrema of the DOG from Equation 6, we use the Normalized Cross-Correlation (NCC) method [9] to establish correspondences between interest points in the image pairs, as shown in Equation 7. Here, we assume that the test image is skewed by only a small angle relative to the master image. We use an $(S + 1) \times (S + 1)$ window around the corner pixel in the master image, and use the same window around the corresponding pixels in the scanned test image. We work with the gray-level versions of both images. We can minimize the NCC to establish correspondences between master and scanned test images.

$$NCC([m_1, m_2]) = \frac{\sum_{i=-S/2}^{S/2} \sum_{j=-S/2}^{S/2} (I_1[i, j] - m_1)(I_2[i, j] - m_2)}{\sqrt{\sum_{i=-S/2}^{S/2} \sum_{j=-S/2}^{S/2} (I_1[i, j] - m_1)^2 \sum_{i=-S/2}^{S/2} \sum_{j=-S/2}^{S/2} (I_2[i, j] - m_2)^2}} \quad (7)$$

In Equation 7, S is the size of the window. I_1 and I_2 are the gray levels of each pair of interest points in both the master and test symbol ROIs. m_1 and m_2 are the average gray level of the windows in the master and test symbol ROIs. The NCC value will be between -1 and 1 . Being 1 means a perfect match between the two interest points within the comparison windows.

The matched interest points are a set of pairs of 2D coordinates. We calculate the geometric matrix to transform the interest points from the test symbol ROI to the corresponding interest points in the master symbol ROI. The 3×3 transformation matrix can remove the skew angle and translation distortion in the test symbol ROI. Four pairs of interest points can solve this matrix. In practice, we prefer to use more matched interest points to get a more accurate transformation matrix. We use the random sample consensus (RANSAC) algorithm [10] to calculate the best transformation matrix. We process the test symbol ROI using the transformation matrix and get the aligned test symbol ROI. Figure 4 (b) shows the blend image of the master and aligned test symbol ROIs. We can find that the text characters in the blue bounding box match better than the same area in the blend image Figure 4 (a). But in the red bounding box, there is still a little misalignment between the master and test text characters. We need to remove this small misalignment, and get a pixel-to-pixel match between the master and test text characters.

3.2 MTB for text characters alignment

After we do the image registration between the master and test symbol ROIs, there is still a small misalignment for some part of the text characters in the test symbol ROI, as shown in Figure 5 (a). We can find there are about 5 to 10 pixels misalignment between the master text characters and the test text characters. We use the median threshold bitmap (MTB) method to align the text characters in each test symbol ROI one-by-one based on the corresponding master symbol ROI [11].



Figure 5: Text characters alignment with the MTB method.

Before using the MTB method, we need to extract the text characters first. We use Otsu's method to extract the text characters from the master and test symbol ROI. Then, based on Otsu's result [12], we use the connected components algorithm to extract each text character bounding box from the master symbol ROI. For each master text character bounding box, we crop out a bigger bounding box at the same position in the test symbol ROI. The bigger bounding box is 20 pixels larger in the x and y direction than the master text character bounding box. We move the master text character bounding box on the test text character bounding box from left to right (x direction) and from top to bottom (y direction). At each moving step, we calculate the difference of these two binary maps in the overlapping area with an exclusive-or (XOR) operator. After processing all the positions, we get the minimum exclusive-or result position. If this position is in the center of the test text character bounding box, there is no misalignment. Otherwise, we calculate the shift in the x and y directions to remove the misalignment between the master and test text characters, as shown in Equation 8. In Equation 8, M is the master text character connected component bounding box binary image; T is the test text character connected component bounding box binary image; $[i, j]$ is the position of the pixels in the binary images; x, y is the pixel shift of the master binary image relative to the test binary image. After processing all the text characters connected components in the test symbol ROI, we will get a text character aligned symbol ROI image, as shown in Figure 5 (b). This result can be used to detect text fading defects according to the following process. This method is much faster than the template matching method because the MTB only uses byte-wise arithmetic.

$$\min_{x,y} Error = \sum_{i,j} XOR(M[i-x, j-y], T[i, j]) \quad (8)$$

4. Text fading detection and classification

In the previous section, the text characters in the test symbol ROI are aligned with the text characters in the master symbol ROI. In this section, we compare and extract the

difference features between the master text characters and test text characters, and then use these features to detect and classify the text fading defect.

4.1 Text fading defect feature vector extraction

The most common way to compare the difference between two different colors is to calculate the ΔE , which is the Euclidean distance between two colors in CIE $L^*a^*b^*$ color space [13]. We calculate the average L^* , a^* , b^* for each text character in the master and test symbol ROIs using Equation 10. Then, we use Equation 9 to calculate the ΔE value for each corresponding text character in the master and test symbol ROIs.

$$\Delta E(t) = \sqrt{(L_{(t)ave}^{master} - L_{(t)ave}^{test})^2 + (a_{(t)ave}^{master} - a_{(t)ave}^{test})^2 + (b_{(t)ave}^{master} - b_{(t)ave}^{test})^2} \quad (9)$$

$$L_{(t)ave} = \frac{\sum_{i=1}^S L(i)}{S}, \quad a_{(t)ave} = \frac{\sum_{i=1}^S a(i)}{S}, \quad b_{(t)ave} = \frac{\sum_{i=1}^S b(i)}{S} \quad (10)$$

In Equation 9, t is the label for a specific text character; $L_{(t)ave}^{master}$ is the average L^* value of the text character t in the master symbol ROI; $L_{(t)ave}^{test}$ is the average L^* value of the text character t in the test symbol ROI; $a_{(t)ave}^{master}$, $a_{(t)ave}^{test}$, $b_{(t)ave}^{master}$, and $b_{(t)ave}^{test}$ conform to the same pattern. In Equation 10, S is the number of pixels in the bounding box for the t text character.

After calculating the ΔE value for each text character, we can get the average ΔE for all the text characters. This average text characters ΔE value is the first feature extracted for text fading detection and classification. Using a similar method, we calculate the ΔE value between the master symbol ROI text characters and the white color, which is (100, 0, 0) in CIE $L^*a^*b^*$ color space. Also, we calculate the ΔE value between the test symbol ROI text characters and the white color. These three ΔE features can be used to classify the text fading defect.

4.2 Text fading defect multi-classification

We classify the text fading defect to four different ranks based on the severity of the text fading defect. Rank A means no text fading defect in the symbol ROIs; Rank B means there is a text fading defect in the symbol ROIs, and the defect does not affect the regular use of the printed page; Rank C means there is an observable text fading defect and people can find it easily; Rank D means there are a lot of text fading defects and the defects influence the regular use of the printed page. Figure 6 shows sample symbol ROIs for the four different ranks.

To train a four ranks multi-classification model, we manually label 120 symbol ROIs as ground truth based on the text fading defect, which includes 30 rank A, 26 rank B, 30 rank C, and 34 rank D. In order to design a more balanced multi-classification model, we apply the Directed Acyclic Graph-Support Vector Machine (DAG-SVM) method [14], which is

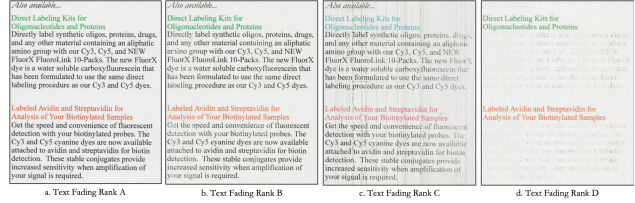


Figure 6: The text fading defect rank sample symbol ROI.

a tree-structured classifier. It is more balanced than the One vs. Rest (OvR) strategy in the training process and more efficient than the One vs. One (OvO) strategy [15]. Figure 7 shows the structure of the DAG-SVM for our four ranks multi-classification process.

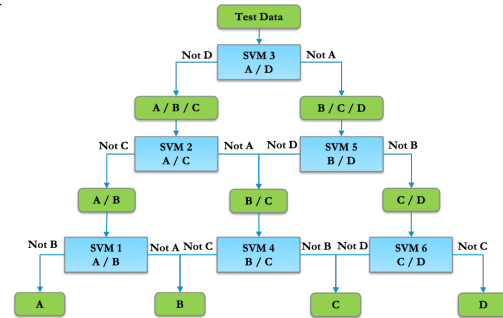


Figure 7: DAG-SVM for text fading defect classification.

To evaluate this multi-classification result, we separate the 120 ground truth symbols ROIs into 5 folds. Each fold includes 24 symbol ROIs, and also each fold includes four ROIs for each rank A/B/C/D. We evaluate the multi-classification model by processing the cross-validation. Each fold will be used as a test set one time, and the other four folds are used as training sets. The final confusion matrix for this five-fold cross-validation is shown in Table 1.2. The accuracy of this multi-classification model is 86.7%, and the standard deviation of the five-fold test accuracy is 12.67% with the worst accuracy 66.7% and the best accuracy 100%.

Table 1: Text fading defect DAG-SVM classification confusion matrix

	Predict A	Predict B	Predict C	Predict D
Real A	26	2	2	0
Real B	0	26	0	0
Real C	2	2	24	4
Real D	0	2	2	28

5. Predict the depleted cartridge

In the previous section, we extracted the text fading defect feature vector and did the rank classification. However, the rank classification only shows the severity of the text fading defect. We do not know which cartridge is low and needs to be replaced. In this section, we design a method to predict the depleted cartridge. Firstly, we use a cluster classification method to classify different color text characters. Then, we calculate the possible depleted cartridge for each cluster of color text characters.

5.1 Classify different color text characters

Before predicting the depleted cartridge, we first need to classify different color text characters, because different color text characters may use different cartridges. For example, the symbol ROIs in Figure 2 (b) include different color text characters: red, green, and black. The red text characters are useful for predicting depletion of the yellow and magenta cartridges, and blue text characters are useful for predicting depletion of the cyan and magenta cartridges. So, we need to detect and classify different color text characters. We do not know the number of colors in one symbol ROI, so we cannot use the K-means algorithm directly. To solve this problem, we use the gap statistic method to calculate the number of colors in the symbol ROI, and then we use the K-means algorithm [16] to classify the different color text characters. We introduce the details in the following part.

Firstly, we need to transform the master symbol ROI and test symbol ROI to CMYK color space. First, the R, G, and B values are divided by 255 to change the range from [0, 255] to [0, 1], as shown in Equation 11.

$$R' = \frac{R}{255}, \quad G' = \frac{G}{255}, \quad B' = \frac{B}{255} \quad (11)$$

Then, the black (K) color is calculated from the red (R'), green (G'), and blue (B') colors, as shown in Equation 12.

$$K = 1 - \max(R', G', B') \quad (12)$$

The cyan (C) color is calculated from the red (R') and black (K) colors, the magenta (M) color is calculated from the green (G') and black (K) colors, and the yellow (Y) color is calculated from the blue (B') and black (K) colors, as shown in Equation 13.

$$C = \frac{1 - R' - K}{1 - K}, \quad M = \frac{1 - G' - K}{1 - K}, \quad Y = \frac{1 - B' - K}{1 - K} \quad (13)$$

This conversion assumes full under-color removal. Also, C , M , and Y are normalized to sum to 1. A more accurate conversion could be based on the color management pipeline within the printer. But this would be printer-dependent, and might even depend on the current calibration state of the printer.

We can extract the pixels of each text character, and we calculate the average values in the C, M, Y, and K channels for each text character for both the master and test symbol ROIs.

We use the gap statistic method and the K-means algorithm to classify the color text characters [17]. The gap statistic method is a method to estimate the number of colors in one symbol ROI. The technique uses the output of the K-means algorithm, comparing the change in within-cluster dispersion with that expected under an appropriate reference null distribution. We calculate the gap from $k = 1$ until $k = 5$, where k is the number of clusters trying to classify the text characters in the symbol ROI based on the data set. Suppose that we have clustered the data into k clusters C_1, C_2, \dots, C_k

with C_r denoting the indices of observations in cluster r , and $n_r = |C_r|$. The sum of the pairwise squared Euclidean distances for all points in cluster r is calculated by Equation 14, and then Equation 15 is used to calculate W_k , which is the pooled within-cluster sum of squares of distance from the cluster means. The sample size n is suppressed in this notation.

$$D_r = \sum_{x_i \in C_r} \sum_{x_j \in C_r} \|x_i - x_j\|^2 \quad (14)$$

$$W_k = \sum_{r=1}^k \frac{1}{2n_r} D_r \quad (15)$$

The idea of the gap statistic is to standardize the graph of $\log(W_k)$ by comparing it with its expectation under an appropriate null reference distribution of the data. The estimate of the optimal number of clusters is then the value of k for which $\log(W_k)$ falls the farthest below this reference curve. We can use the maximum value of Equation 16 to find the optimal number of clusters for the color text characters. In Equation 16, E_n^* denotes expectation under a sample of size n from the reference distribution. The optimal estimate for k will be the value maximizing $Gap_n(k)$ after we take the sampling distribution into account.

$$Gap_n(k) = E_n^* \{ \log(W_k) \} - \log(W_k) \quad (16)$$

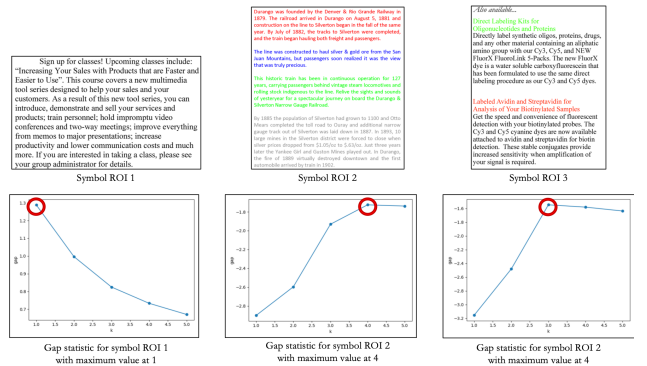


Figure 8: Three examples illustrating the use of the gap statistic to detect the optimal number of clusters for color text characters in one symbol ROI.

We apply this gap statistic method for the color text characters to detect the optimal number of color clusters for one symbol ROI. Three example symbol ROIs and their corresponding gap statistic plots from $k = 1$ to $k = 5$ are shown in Figure 9. In Figure 9, each symbol ROI includes a different number of colors of its text characters, and the gap statistic takes on its maximum value at the value for k that equals the number of colors in the corresponding symbol ROI.

5.2 Predict the depleted cartridge

After we know the optimal number of clusters for the color text characters in one symbol ROI, we can use the K-means algorithm to classify the text characters, and each

cluster includes the same color text characters, as shown in Figure 9 (a). This will be very useful to detect the depleted cartridge. For each text character color in the master symbol ROI, we can extract the same color corresponding text characters from the test symbol ROI, and calculate the average C_{test} , M_{test} , Y_{test} , and K_{test} values, as shown in Figure 9 (b). In our algorithm, the C , M , Y , and K values range from 0 to 1. If the error between the master color channel value and the corresponding test color channel value is more than 0.1, the corresponding cartridge is depleted. For example, in Figure 20, the cartridge that is predicted to be depleted is the magenta cartridge.

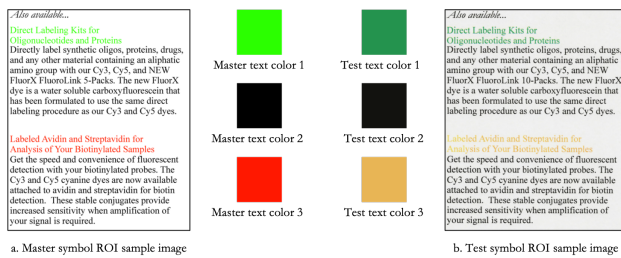


Figure 9: The text colors extracted from the master symbol ROI.

6. Conclusion

In this paper, we proposed a text fading defect detection and classification method. The input consists of master symbol ROIs and the corresponding test symbol ROIs. And the output is the text fading defect feature vector, rank classification, and the predicted empty cartridge. To achieve this result, we design three parts in our procedure: text character alignment, text fading classification, and prediction of the depleted cartridge. In the first part, we use an image registration algorithm to align the test symbol ROI based on the master symbol ROI. Then, we use the median threshold bitmap algorithm to do the text character alignment. In the second part, we transform the color space to CIE $L^*a^*b^*$ and extract the ΔE value between the master and test text characters. We deploy these useful features to classify the rank of the text fading defect in the test symbol ROI. In the third part, we first calculate the number of text colors in one symbol ROI, and for each color, we extract the master text characters and the corresponding test text characters. We transform these text characters to CMYK color space, and compare the difference between the average text color values in the master and test ROIs to predict the depleted cartridge.

References

- [1] Y. Ju, R. J. Jessome, E. Maggard, and J. P. Allebach, "Autonomous Detection of Text Fade Point with Color Laser Printers," *International Society for Optics and Photonics, Image Quality and System Performance XII*, San Francisco, CA, 8 February 2015.
- [2] Z. Xiao, S. Xu, E. Maggard, K. Morse, M. Shaw and J. P. Allebach, "Detection of Color Fading in Printed Customer Content," *Electronic Imaging, Color Imaging XV: Image Quality and System Performance*, Burlingame, CA, January 2018.

- [3] R. Zhang, Y. Yang, E. Maggard, Y. Bang, M. Cho, and J. P. Allebach, "A Comprehensive System for Analyzing the Presence of Print Quality Defects," *Electronic Imaging, Image Quality and System Performance XVII*, San Francisco, CA, 26 January 2020.
- [4] R. Zhang, E. Maggard, Y. Bang, M. Cho, and J. P. Allebach, "Region of interest extraction for image quality assessment," *Electronic Imaging, Image Quality and System Performance XVII*, San Francisco, CA, 26 January 2020.
- [5] A. Vavilin and K-H. Jo, "Fast HDR Image Generation from Multi-exposed Multiple-view LDR Images," *3rd European Workshop on Visual Information Processing*, Paris, France, 4 July 2011.
- [6] H. Foroosh, J.B. Zerubia, and M. Berthod, "Extension of Phase Correlation to Subpixel Registration," *IEEE Transactions on Image Processing*, 7 August 2002.
- [7] D.G. Lowe, "Object Recognition from Local Scale-invariant Features," *Proceedings of the Seventh IEEE International Conference on Computer Vision*, Kerkyra, Greece, 6 August 1999.
- [8] S. R. Gunn, "On the discrete representation of the Laplacian of Gaussian," *Pattern Recognition*, 1 August 1999.
- [9] F. Zhao, Q. Huang, and G. Wen, "Image Matching by Normalized Cross-Correlation," *2006 IEEE International Conference on Acoustics Speech and Signal Processing Proceedings*, Toulouse, France, 14-19 May 2006.
- [10] M. A. Fischler, and R. C. Bolles, "Random Sample Consensus: A Paradigm for Model Fitting with Applications to Image Analysis and Automated Cartography," *Communications of the ACM*, Toulouse, France, 1 June 1981.
- [11] K. Jacobs, C. Loscos, and G. Ward, "Automatic High-Dynamic Range Image Generation for Dynamic Scenes," *IEEE Computer Graphics and Applications*, 03 March 2008.
- [12] L. Di Stefano and A. Bulgarelli, "A Simple and Efficient Connected Components Labeling Algorithm," *IEEE, Proceedings 10th International Conference on Image Analysis and Processing (pp. 322-327)*, September, 1999.
- [13] R. Zhang, E. Maggard, R. Jessome, Y. Bang, M. Cho, and J. P. Allebach, "Block Window Method with Logistic Regression Algorithm for Streak Detection," *Electronic Imaging, Image Quality and System Performance XVI*, Burlingame, CA, January 2018.
- [14] P. Chen, and S. Liu, "An Improved DAG-SVM for Multiclass Classification," *2009 Fifth International Conference on Natural Computation*, Tianjian, China, 14-16 August. 2009
- [15] D.M.J. Tax, and R.P.W. Duin, "Using two-class classifiers for multiclass classification," *IEEE, Object Recognition Supported by User Interaction for Service Robots*, Quebec City, QC, Canada, 11 August 2002.
- [16] K. Krishna, and M. N. Murty, "Genetic K-means algorithm," *IEEE Transactions on Systems*, June 1999.
- [17] R. Tibshirani, G. Walther, and T. Hastie "Estimating the Number of Clusters in A Data Set Via the Gap Statistic," *Journal of the Royal Statistical Society*, 06 January 2002.

Author Biography

Runzhe Zhang received his B.S. degree in Mechanical Engineering from Qingdao University of Technology (2013), Shandong, China and received the M.S. degree in Mechanical Engineering from Boston University, MA, USA. Currently, he is pursuing the Ph.D. in Electrical and Computer Engineering at Purdue University. His research areas include digital image processing, computer vision, and machine learning.

Eric Maggard received his B.S. degree in Physics from Northwest Nazarene University, Nampa, Idaho in 1991 and the M.S. degree in Computer Science specializing in image analysis and processing from Walden University in 2006. He is an Expert Imaging Scientist in the LaserJet Hardware Division and has developed programs and image quality algorithms for the last 15 years that are used in the testing of LaserJet print and scan image quality. His interests include machine vision, object recognition, machine learning, robot control, and navigation.

Yusun Bang is a manager of Image Quality Part in the Imaging Lab at HP Printing Korea Co. Ltd. She received her BS and MS in mathematics from Ewha Womans University, Seoul, Korea in 1994 and 1996, and her Ph.D. in the School of Electrical and Computer Engineering, Purdue University, West Lafayette, Indiana in 2005. She worked for Samsung Advanced Institute of Technology and Samsung Electronics Company from 2004 to 2017. Her current research interests include image quality diagnosis and metrics and ML/DL based prediction for smart device services.

Minki Cho is an engineer with HP Printing Korea. He received B.S.(1997) and M.S.(1999) in electrical engineering from the Inha University, Korea. From 2003 to 2017, he worked for Samsung Electronics and Samsung Advanced Institute of Technology. His research areas are print image processing, print image quality diagnosis and calibration. Recently, he is researching the above interests using ML and DL.

Mark Shaw received his B.S. in Printing and Publishing Technology from University of Herfordshire in 1997 and his M.S. in Color Science from Rochester Institute of Technology in 1999. Then he went to Boise State University to take Electrical Engineering classes to meet the pre-requisites to study under Prof. Jan Allebach at Purdue. Finally he received his Ph.D. in Electrical and Computer Engineering from Purdue University in 2015. He is now a principal color and imaging master architect at HP Inc.

Jan P. Allebach is Hewlett-Packard Distinguished Professor of Electrical and Computer Engineering at Purdue University. Jan P. Allebach is a Fellow of the IEEE, the National Academy of Inventors, the Society for Imaging Science and Technology (IS&T), and SPIE. He was named Electronic Imaging Scientist of the Year by IS&T and SPIE and was named Honorary Member of IS&T, the highest award that IS&T bestows. He has received the IEEE Daniel E. Noble Award, the IS&T/OSA Edwin Land Medal, the IS&T

Johann Gutenberg Prize, and is a member of the National Academy of Engineering.

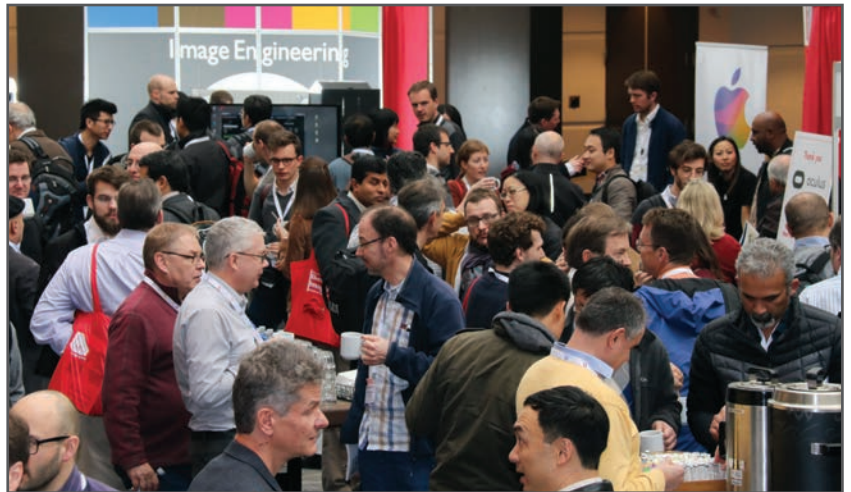
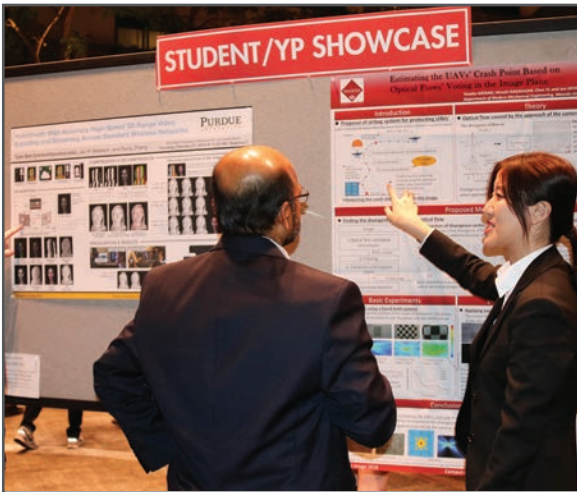
JOIN US AT THE NEXT EI!

IS&T International Symposium on

Electronic Imaging

SCIENCE AND TECHNOLOGY

Imaging across applications . . . Where industry and academia meet!



- **SHORT COURSES • EXHIBITS • DEMONSTRATION SESSION • PLENARY TALKS •**
- **INTERACTIVE PAPER SESSION • SPECIAL EVENTS • TECHNICAL SESSIONS •**

www.electronicimaging.org

